Photosynthesis Research (2022) 152:297–304
https://doi.org/10.1007/s11120-021-00895-3

ORIGINAL ARTICLE

Psb27, a photosystem II assembly protein, enables quenching of excess light energy during its participation in the PSII lifecycle

Virginia M. Johnson[1] · Sandeep Biswas[1] · Johnna L. Roose[2] · Himadri B. Pakrasi[1] · Haijun Liu[1]

Received: 4 October 2021 / Accepted: 27 December 2021 / Published online: 5 January 2022

Abstract

Photosystem II (PSII), the enzyme responsible for oxidizing water into molecular oxygen, undergoes a complex lifecycle during which multiple assembly proteins transiently bind to and depart from PSII assembly intermediate complexes. Psb27 is one such protein. It associates with the CP43 chlorophyll-binding subunit of PSII to form a Psb27-PSII sub-complex that constitutes 7–10% of the total PSII pool. Psb27 remains bound to PSII assembly intermediates and dissociates prior to the formation of fully functional PSII. In this study, we compared a series of Psb27 mutant strains in the cyanobacterium *Synechocystis* sp. PCC 6803 with varied expression levels of Psb27: wild type (WT); *psb27* genetic deletion (Del27), genetically complemented *psb27* (Com27); and over-expressed Psb27 (OE27). The Del27 strain demonstrated decreased non-photochemical fluorescence quenching, while the OE27 strain showed increased non-photochemical quenching and tolerance to fluctuating light conditions. Multiple flashes and fluorescence decay analysis indicated that OE27 has the least affected maximum PSII quantum yield of the mutants. OE27 also displayed a minimal impact on the half-life of the fast component of Q_A^- reoxidation over multiple flashes, indicating robust PSII function. We propose that the close association between Psb27 and CP43, and the absence of a fully functional manganese cluster in the Psb27-PSII complex create a PSII sub-population that dissipates excitation energy prior to its recruitment into the functional PSII pool. Efficient energy dissipation prevents damage to this pre-PSII pool and allows for efficient PSII repair and maturation. Participation of Psb27 in the PSII life cycle ensures high-quality PSII assembly.

Keywords Photosystem II · Photosynthesis · Non-photochemical quenching · *Synechocystis* 6803

Introduction

Photosystem II (PSII) is a unique enzyme in that it routinely experiences damage caused by one of its substrates, light, and its derivative reactive oxygen species. Additionally, PSII is assembled modularly from chlorophyll-containing subunits, which themselves are sensitive to damage by absorption of light prior to complete PSII assembly. On the organismal level, this photodamage is detrimental to fitness unless a protective mechanism is adopted to dissipate excess light energy, both during assembly and under photoactive conditions. Cyanobacteria have several known mechanisms of excitation energy quenching and redistribution, collectively called non-photochemical quenching (NPQ). These include quenching via the orange carotenoid protein (OCP), which, in its light-induced active state, uncouples the excitation energy transfer from phycobilisome antennas to PSII, reducing its functional cross section (Wilson et al. 2006; Wilson et al. 2008). Another mechanism is via IsiA, a chlorophyll-containing homolog of CP43, which forms oligomeric ring structures under stress conditions (Chen et al. 2018; Ihalainen et al. 2005). These rings are thought to absorb and dissipate excess light energy as a means of photoprotection. Additionally, during assembly, the reaction center proteins of PSII are associated with carotenoid-containing quenching proteins known as HLIPS for protection prior to their assembly into active PSII (Knoppova et al. 2014; Niedzwiedzki et al. 2016). This mechanism relies on carotenoids' ability to quench both triplet chlorophyll and singlet oxygen. Cyanobacteria have two other mechanisms

✉ Himadri B. Pakrasi
pakrasi@wustl.edu

[1] Department of Biology, Washington University in St. Louis, St. Louis, USA

[2] Division of Biochemistry and Molecular Biology, Department of Biological Sciences, Louisiana State University, Baton Rouge, LA, USA

of fluorescence quenching and redistribution. These are state transitions, which regulate the distribution of excitation energy between PSII and PSI, and photoinhibition, which results from the high-light-induced inactivation of PSII caused by damage and degradation of the D1 protein.

Elucidation of photoprotective strategies that occur at the molecular level promises to inspire rational redesign of photosynthesis to sustainably meet current and future global food and energy demand (Ort et al. 2015). Recently, increasing the responsiveness of photoprotective quenching routes to fluctuating light conditions has been observed to have a significant (15%) positive impact on crop yield under simulated field conditions (Kromdijk et al. 2016). Overall, the increased availability of protective quenchers and accelerated recovery from NPQ in lower light conditions allowed for increased environmental adaptability and thus increased photosynthetic productivity.

Psb27, a small extrinsic membrane protein, is only bound to inactive PSII. It binds either to monomeric PSII during de novo assembly and repair, or to dimeric PSII during repair (Nowaczyk et al. 2006; Grasse et al. 2011; Liu et al. 2011a, b, c; Singh 2017). It is thought to enable the efficient light-driven assembly (photoactivation) of the Mn cluster (Roose and Pakrasi 2008; Avramov et al. 2020). In strains lacking Psb27, PSII can assemble fully, but photoactivation is slower and recovery from photodamage is slower as well (Roose and Pakrasi 2008; Jackson et al. 2014; Davinagracia 2021). In the absence of both Psb27 and CP47, unassembled CP43 is degraded at a higher rate (Komenda et al. 2012), which indicates that Psb27 stabilizes CP43 and allows a relatively larger amount of the pre-complex (Psb27-CP43) to form. Psb27 is not found in the structure of active PSII, but recently, structures of PSII assembly complexes bound to Psb27 have been elucidated using cryo-electron microscopy (Zabret et al. 2021), (Huang et al. 2021). These structures reveal that Psb27 binds to the surface of Loop E of CP43 distal to the Mn-binding site, or D1/D2 axis, which is consistent with two previous observations from mass spectrometry crosslinking and protein foot-printing (Liu et al. 2011a, b, c; Liu et al. 2013). These findings have suggested an allosteric role of Psb27 in maintaining PSII in a nonfunctional state, ready for the final steps of PSII assembly. However, the details of such structural arrangements remain unclear.

Psb27 is conserved across all oxygenic photosynthetic organisms. In *Arabidopsis thaliana*, Psb27 is not essential for PSII formation and photoautotrophic growth. The absence of Psb27, however, leads to decreased recovery of the photodamaged PSII complex (Chen et al. 2006), especially in fluctuating light (Hou et al. 2015). We suggest that a similar growth benefit may be conferred by Psb27 in cyanobacteria, and we propose a mechanistic explanation for how Psb27-PSII contributes to optimal PSII function and eco-physiological fitness in cyanobacteria.

Results

This study analyzed four strains of *Synechocystis* sp. PCC 6803 for growth and photosynthetic parameters: WT, a deletion mutant of Psb27 (Del27), a strain complementing the deletion (Com27), and a weak overexpression line of Psb27 (OE27). Figure 1A shows the growth rates of these strains under standard lab conditions: constant, low-level (30 µM photons m^{-2} s^{-2}) light. Figure 1B shows the growth rate under fluctuating light conditions: a 30-min-high light/30-min dark cycle. While the growth rates are quite similar, the OE27 strain under continuous light shows slower initial growth before catching up to the WT at about 4–5 days of growth. Under fluctuating light conditions, the growth rate of the strains is similar as well, but the OE27 strain overtakes the WT after several days of growth. Interestingly, under fluctuating light, the Del27 strain and Com27 strains also appear to overtake the WT.

To further test the photosynthetic parameters of these strains, cells were grown on BG11 plates without antibiotics

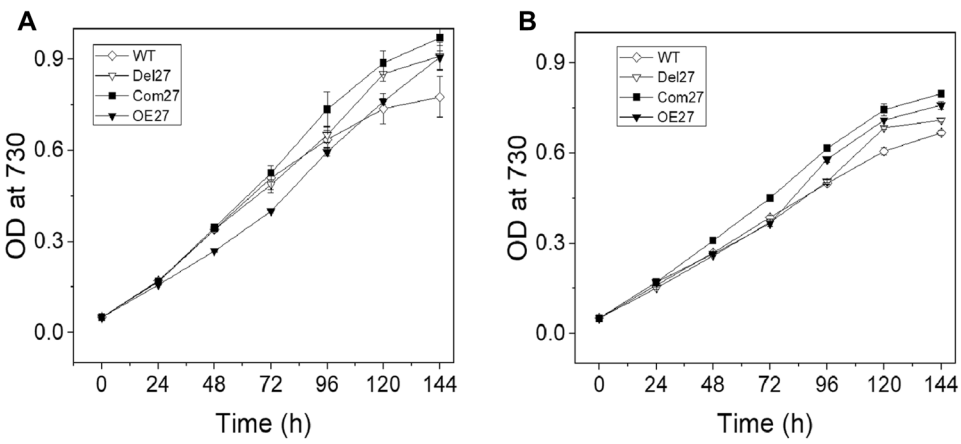

Fig. 1 OE27 growth outpaces WT *Synechocystis* 6803 in fluctuating light. **A** Growth under continuous light. This figure shows the growth curve of WT, Del27, Com27, OE27 under normal growth continuous light (30 µmol photons/m^2s^1). **B** Growth under 1200 µmol photons/m^2s^1, 30 min of on–off cycles

and the Fluorocam 800MF was used to assay for non-photochemical quenching. Figure 2A shows the NPQ trace collected for each of the four strains. Application of a saturating pulse to the dark-adapted plate induced a maximum value of fluorescence, *F*m, by closing reaction centers, at that time there was no NPQ because the colonies had been fully dark-adapted. Following a dark relaxation, a sufficiently strong actinic light was applied and an initial rise in fluorescence was observed. This fluorescence was then partially quenched as a result of increasing competition with photochemical and non-photochemical events. Five saturating pulses were applied under actinic illumination that transiently closed all the reaction centers and provided a value of maximal fluorescence in the light-adapted state, termed *F*m′. The difference between *F*m and *F*m′ is due to the contribution of NPQ. Figure 2B plots the plant vitality index, Rfd, derived from peak fluorescence, *F*m, attained during the first seconds of the transient, and the steady-state fluorescence, *F*s, in the light-adapted phase. In healthy photosynthetic cells, there is a larger value, as shown for WT and Com27, while Del27 has a slower rise than WT. Conversely, OE27 demonstrates an accelerated rise which means that this strain's overall physiological fitness is increased. Figure 2C shows the coefficient of photochemical quenching during actinic light conditions, which reflects the process of photosynthesis itself. Upon light illumination, enzymes in the Calvin–Benson Cycle activate fully, the metabolite pool size increases, and the carbon concentrating mechanism for feeding CO_2 to Rubisco is initiated. These factors lead to an increased electron sink from the photosynthetic electron transport chain and contribute to quenching. To our surprise, Del27 showed effectively no increase in the time range recorded, and WT and Com27 showed a gradual increase, in parallel with that of OE27. The values for WT and Com27, however, are less than that of the OE27. Figure 2D shows the NPQ recorded during the actinic and dark phases, derived from the difference of *F*m and *F*m′. OE27 has the highest NPQ levels, in contrast to the lowest level in Del27, with WT and Com27 in between.

Figure 3 shows Q_A^- reoxidation over 1000 flashes. Before the measurement, we performed dark-adapted fluorescence induction analysis, known as Kautsky induction (Fig. 3A). The dark-adapted *F*v/*F*m values of the four strains are comparable. This is the basis for NPQ and the following fluorescence kinetics analysis. The 'multiple flashes' experiment is modified from the S-state program equipped in the FL-200 fluorometer. It is a sequence of 1000 saturating flashes over the course of 500 s (see "Materials and Methods"). We used multiple flashes to compare the charge recombination of the dark-adapted strains after a single flash and its associated S-state, and to compare the first charge recombination with recombination after multiple flashes. Each flash also contributes to the redox state of PSII and thus the thylakoids overall, so the observed values reflect the redox state changes after actinic light illumination over a longer time scale (> 5 s). Figure 3B compares the fluorescence decay

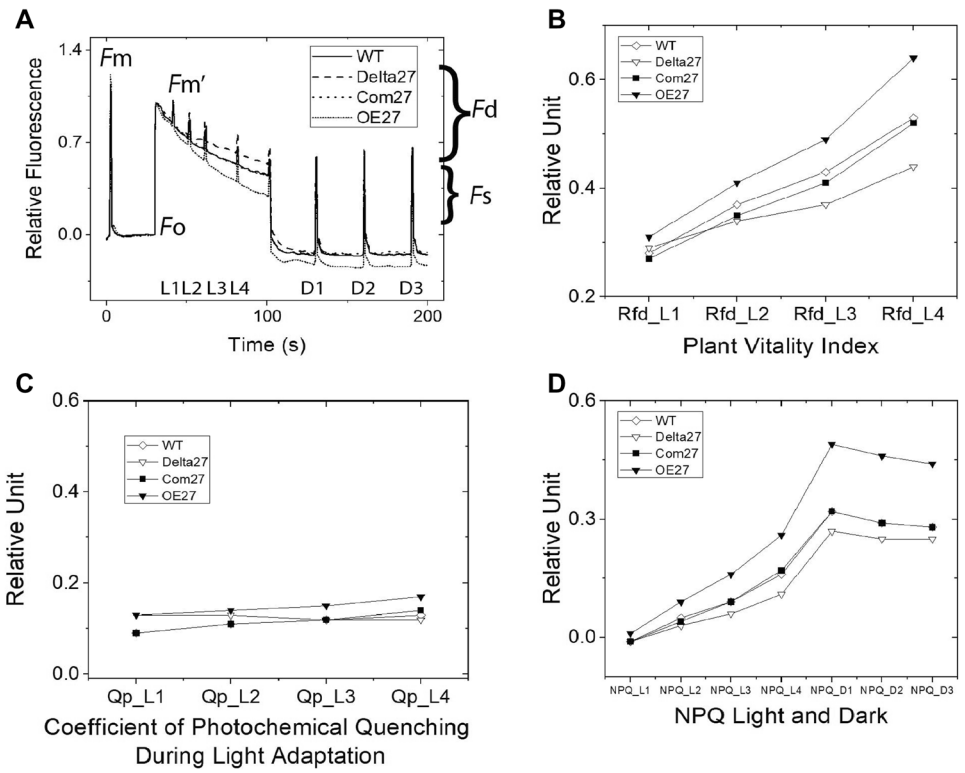

Fig. 2 NPQ is increased in the Psb27 overexpression strain **A** NPQ traces from Fluorocam 800MF of four cell lines. Light and dark schemes are indicated with saturating pulses applied. *F*m, *F*d, and *F*s are marked for WT trace. Deconvolution of the traces followed manufacturer's protocol (Photo System Instruments, Brno, Czech Republic). **B** Plant vitality index Rfd (*F*d/*F*s) at intervals during light exposure. **C** Coefficient of quenching (*F*m′−*F*)/(*F*m′−*F*o′). **D** NPQ ((*F*m−*F*m′)/*F*m′). Data are representative of three replicates

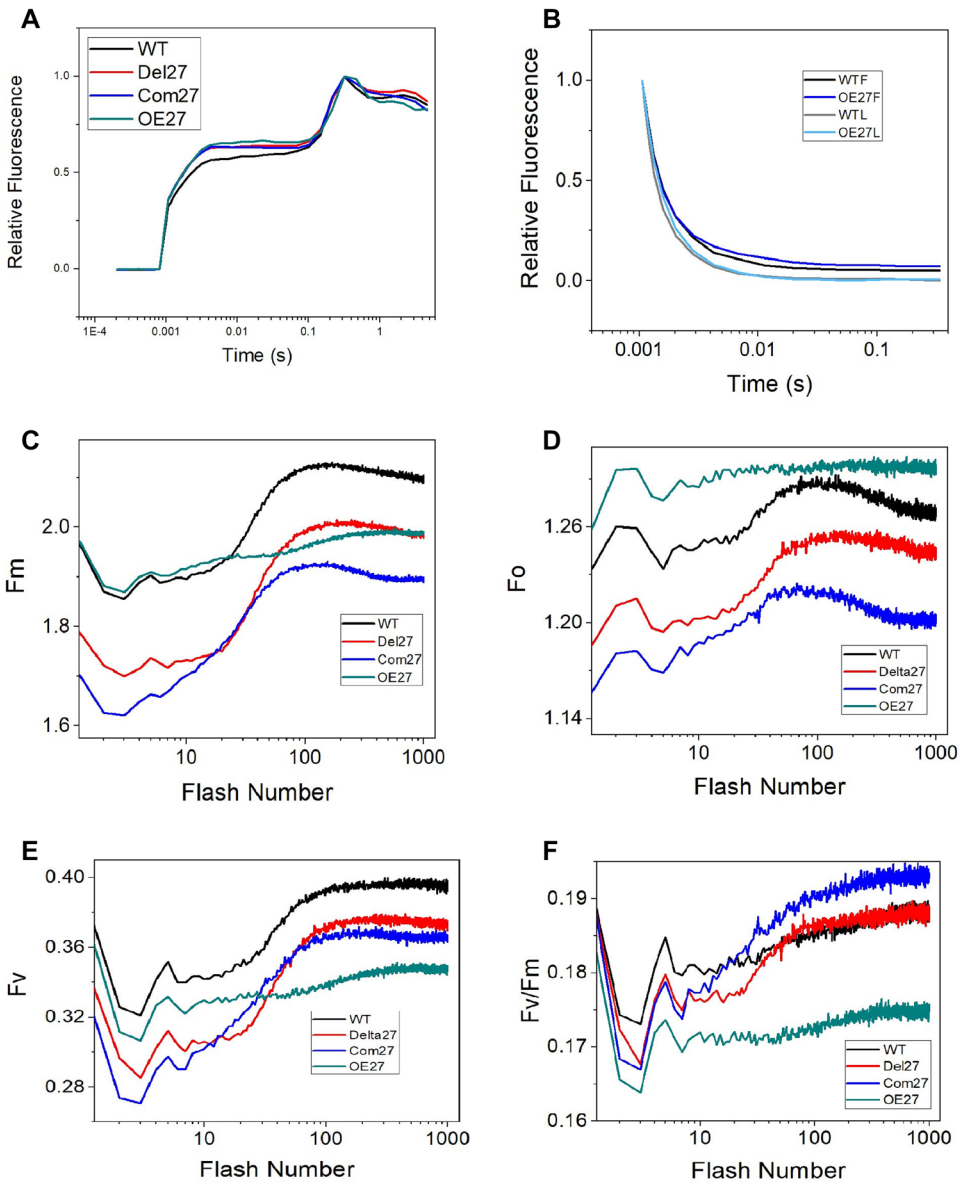

Fig. 3 OE27 is resilient to light adaptation over 1000 flashes. **A** Fluorescence induction (Kautsky effect), **B** Fluorescence decay over 500 ms for WT and OE27 strains after first (F) and last (L, 1000) flashes. **C** *F*m fluctuation over 1000 flashes. **D** *F*o fluctuation over 1000 flashes. **E** *F*v derived from (**C**) and (**D**). *F*v value shows periodic change which is the opposite of flash-induced oxygen yield. Some studies use these values to derive S-state distribution analysis. **F** *F*v/*F*m maximum quantum yield of PSII chemistry

after the first and last (1000) of the flashes for WT and OE27 (data of Del27 and Com27 are not shown for clarity), which is driven by charge transfer from the plastoquinone Q_A to Q_B in the PSII electron transport chain. To model the charge transfer kinetics between Q_A^- and the plastoquinone bound at the Q_B-binding site, we employed a double exponential decay. The fast exponential component describes the charge transfer between Q_A^- and plastoquinone bound at the Q_B site. The second exponential, intermediate, component describes plastoquinone exchange at the Q_B-binding site (Vass et al. 1999). Because the fluorescence decay was recorded for approximately 330 ms after the actinic flash (instrument intrinsic function), we did not consider a slow hyperbolic component ($T_{1/2}$ ranging in seconds) that would describe the $S_2Q_A^-$ charge recombination (Biswas and Eaton-Rye 2018).

Tables 1 and 2 show the decay kinetics for all strains for the first and last flashes (data are in Table S2). Residuals for the fits are shown in Fig S2.

The fluorescence decay kinetics for the fast and intermediate components after a single saturating flash are

Table 1 Fluorescence decay kinetics after a single actinic flash

Strains and treatment	Fast component		Intermediate component	
	Amplitude (%)	$T_{1/2}$ (µs)	Amplitude (%)	$T_{1/2}$ (µs)
WTF	59.1	252.7	40.9	2.1
Del27F	60.5	273.2	39.5	2.2
Com27F	65.6	229.7	34.4	2.2
OE27F	68.0	237.9	32.0	2.6

Table 2 Fluorescence decay kinetics after 1000 actinic flashes

Strains and treatment	Fast component		Intermediate component	
	Amplitude (%)	$T_{1/2}$ (μs)	Amplitude (%)	$T_{1/2}$ (μs)
WTF	39.2	178.8	60.8	1.3
Del27F	42.4	195.1	57.6	1.3
Com27F	43.3	179.8	56.7	1.2
OE27F	50.2	243.9	49.8	1.6

nearly the same for all the strains. However, after 1000 saturating flashes, the $T_{1/2}$ and amplitude for the fast component are considerably different for the OE27 strain compared to other strains (Table 2). The $T_{1/2}$ for the intermediate components for all the strains remain similar. The changes in the amplitudes for the intermediate component between the first flash and thousandth flash would suggest increased photochemistry owing to cells transitioning from dark-adapted to steady-state conditions. After multiple saturating flashes, an overall increase in the electron transfer is also evident from a decline in the half-times of both the fast and intermediate components.

Because Psb27 is not found in active cyanobacterial PSII (Suga et al. 2015) (Nowaczyk et al. 2006; Liu et al. 2011a, b, c), deletion of Psb27 has a minimal impact on the PSII-associated electron-transfer processes as compared to WT (Tables 1 and 2), as expected. The minimal impact on the $T_{1/2}$ for the fast component in the OE27 strain could indicate the robustness of PSII. However, because Psb27 is not a component of active PSII, we hypothesize that more of the Psb27-bound PSII assembly intermediate is available in the OE27 strain. Increased Psb27 assures high quality, efficient PSII assembly based on the previous functional analysis (Roose 2008, Jackson et al. 2014). Under steady-state conditions, an increase in damage to PSII would make PSII maturation in the OE27 strain more efficient than in the other strains and thus a minimal impact on the electron-transfer kinetics is observed, as it is more reflective of new complex formation than adapting PSII centers to light.

Although the fit of the model employed to fit fluorescence decay was satisfactory ($R^2 = 0.99$), the sinusoidal pattern observed for the residuals (Figure S2) would suggest that a model employing a double exponential does not fully describe the relaxation processes taking place. We also did not consider the slow hyperbolic component for curve fitting, which could be contributing to the structure of the residuals.

Figure 3C shows *F*m changes over 1000 saturating flashes. OE27 shows less increase in *F*m than other strains, indicative of either a robust non-photochemical quenching, or NPQ, consistent with the results from Fig. 2C. Figure 3D shows *F*o changes over 1000 flashes. Figure 3E shows *F*v over the 1000 flashes, and Fig. 3F shows *F*v/*F*m. Overall, OE27 shows less of a change over the 1000 flashes than the other strains.

Discussion

In our previous study (Liu et al. 2011a, b, c), we demonstrated that within the PSII population, there is always a sub-population (7–10%) of monomeric Psb27-PSII. This population is characterized by loosely bound PsbO and the absence of a functional Mn cluster, and has severely defective Q_A^- reoxidation by forward electron transfer to Q_B. Fluorescence decay profiles in both Psb27-PSII (His27PSII) and Psb27-Δ*ctpA*PSII (His27Δ*ctpA*PSII) samples without DCMU treatment are similar to those treated with DCMU, an electron transport inhibitor that binds to the Q_B site. Compared with functional PSII (HT3-PSII), forward electron transfer from Q_A^- to Q_B in both Psb27-PSII and Psb27-Δ*ctpA*PSII is blocked, which has been observed previously (Mamedov et al. 2007). The results presented in this work demonstrate that Psb27-PSII is not only involved in PSII assembly, but also correlated with a photoprotective energy-dissipation mechanism. It is thought that the removal of the Mn cluster results in a rise of the redox potential of Q_A–, rendering electron transfer to Q_B less efficient and promoting direct relaxation of Q_A– without forming the triplet state of chlorophyll, a precursor of harmful singlet oxygen (Krieger-Liszkay et al. 2008; Rutherford et al. 2012; Kato et al. 2016).

In the absence of Psb27-PSII in Del27 cells of *Synechocystis* sp. PCC 6803, the NPQ analysis demonstrated the absence of a fluorescence quenching component. This phenotype is fully complemented in Com27 (Fig. 2A), which indicates that the Psb27-PSII protein complexes present in WT comprise a PSII quenching pool. In the overexpression strain of Psb27, non-photochemical quenching parameters are even higher than in WT *Synechocystis* sp. PCC 6803 (Fig. 2A and D). This finding supports the hypothesis that the Psb27-PSII sub-population is involved in energy quenching and that the pool size can be modified by genetically controlling levels of Psb27. We propose that the altered conformation of Loop E of CP43 that is conferred by Psb27 binding contributes to the rearrangement of cofactors (carotenoids, chlorophylls, plastoquinone) that enables the quenching capability of Psb27-PSII (Mamedov et al. 2007; Liu et al. 2013; Huang et al. 2021; Zabret et al. 2021). Psb27-bound PSII lacks a functional Mn cluster and has an altered low-temperature chlorophyll fluorescence profile at 77 K (Nowaczyk et al. 2006; Liu et al. 2011a, b, c), but the relation of these phenomena to enhanced non-photochemical quenching in Psb27-PSII requires further research.

In Fig. 3, we observed the behavior of PSII fluorescence induction and relaxation over the course of 1000 saturating flashes. We showed that OE27 shows less of a change over

time as compared with the WT strain, indicating a higher resilience to light-induced change, and larger pool of PSII assembly complexes in this strain.

We propose a model for Psb27 as an agent of non-photochemical quenching of excitation in PSII assembly and repair intermediates in cyanobacteria (Fig. 4). Increased Psb27 levels lead to an increased pool of Psb27-PSII, ready to mature into active PSII as damage takes place or more PSII is needed, such as in a denser growth condition. This larger pool of non-photosynthetically active PSII can absorb light energy, dissipates it so as not to damage the protein subunits before PSII can function. Interestingly, Bentley et al. (2008) found that the ΔPsb27 strain had a higher rate of oxygen evolution following high light stress, indicating that quenching species are not present, raising the apparent rate compared to chlorophyll content. Our data are consistent with a model of Psb27 expression as the determining factor controlling the amount of Psb27-PSII intermediate complexes, which can quench excitation. It has been shown in previous work that PSII decouples from phycobilisome excitation energy transfer prior to manganese cluster assembly (Hwang et al. 2008). It was also shown that, in the absence of PsbU, an extrinsic PSII subunit binds following manganese (Veerman et al. 2005). Our findings contribute another analogous strategy of the phenomenon decoupling excitation energy prior to full activation of PSII in order to prevent damage.

Cyanobacteria, in particular *Synechocystis* sp. PCC 6803, are widely used to study photosynthesis. However, unlike plants, cyanobacteria used for photosynthesis research are usually grown under continuous light conditions in a constant-temperature growth chamber. In nature, these conditions are nonexistent. Not only are there night/day cycles of light and dark, but during the day light fluctuates due to variable shading caused by wind blowing tree branches, and current movement in a water column. An adaptive photoprotective mechanism under such conditions would have a more significant impact on eco-physiological fitness. We suggest that this is why the quenching function of Psb27 in cyanobacteria has been overlooked until now. A more pronounced phenotype may be evident in a stronger overexpression strain, or with different varying light schemes other than the 30 min of on/off cycle tested in this work. It is also likely that there are conditions under which over-expressing Psb27 is not advantageous, and the current level is a balance between a beneficial quenching state, and an over-protective mechanism.

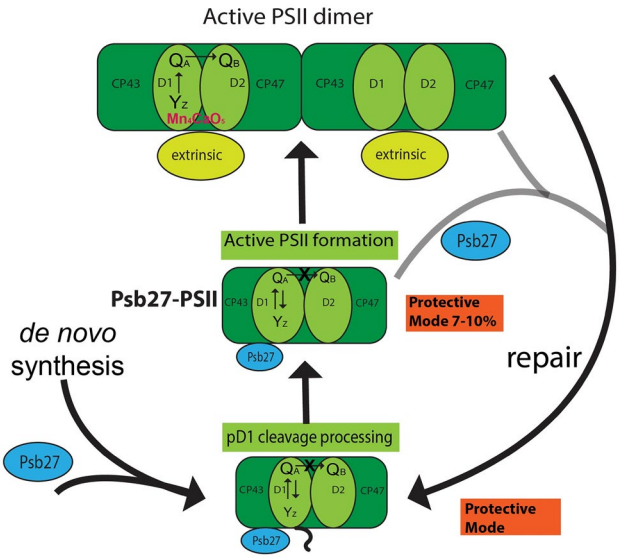

Fig. 4 Schematic of the role of Psb27 NPQ. Psb27 is the determining factor in the pool size of Psb27-PSII from both the synthesis and repair pathways. A larger pool of the quenching species Psb27-PSII forms when more Psb27 is present in the cell, which enables higher NPQ

Materials and methods

Culture and growth of *Synechocystis* sp. PCC 6803 strains

Wild type (WT), Psb27 deletion (Del27) (Roose and Pakrasi 2008), Psb27 complemented (Com27), and Psb27 Overexpression (OE27) of *Synechocystis* 6803 were grown in BG11 medium (Allen 1968) at 30 °C under 30 µmol photons m^{-2} s^{-1}. The genetically modified strains were grown in BG11 supplemented with antibiotics as follows: 5 µg/mL chloramphenicol (Del27), 5 µg/mL chloramphenicol, 2 µg/mL gentamicin (Com27), and 2 µg/mL gentamicin (OE27). For growth assays in liquid medium, cells were grown to mid-log phase, harvested by centrifugation, washed in fresh BG11, and again centrifuged to pellet. The cell pellets were resuspended and diluted to $OD_{730}=0.05$ in BG11 without antibiotics and grown with shaking (200 rpm). The OD_{730} was measured every 24 h on a µQuant Microplate spectrophotometer (Biotek Instruments).

Mutant construction and Psb27 quantification

A complemented strain of the Δ*psb27* (Com27) was generated by inserting a copy of the psb27 locus (*slr1645*) containing 200 bp of upstream and downstream DNA and the coding region of the *slr1645* gene into the *psbA1* locus, a gene that is not expressed under lab growth conditions (Fig. S1A) (Mohamed and Jansson 1989) in the Del27 mutant background (Roose 2008; Roose and Pakrasi 2008). Briefly, psbA1 upstream and downstream DNA fragments were amplified using primers listed, respectively, in Table S1. The *psb27* DNA fragment was amplified using primer pair Psb27Comp5 and Psb27Comp3. Segregation of the modified psbA1 locus was verified by PCR analysis using A1segF and A1segR primers (Fig. S1B). The OE27 was generated

by using the same construct as in Com27, with *psb27* under the native promoter, but introduced into the WT background. All primer sequences are listed in Table S1.

Cyanobacterial cells were harvested and broken by bead beating as described previously (Kashino et al. 2002) with minor modifications. Cells were resuspended in RB buffer (25% glycerol (wt/vol), 10 mM $MgCl_2$, 5 mM $CaCl_2$, 50 mM MES buffer pH 6.0), and broken by vortexing with 0.17 mm glass beads. Membrane fraction was isolated by centrifugation, resuspended in RB, and solubilized by addition of β-D-dodecyl maltoside (DDM) to a final concentration of 0.8%. After incubation on ice in dark for 30 min, the solubilized membranes were separated from the insoluble material by centrifugation at gradually increasing speed from 120×*g* to 27,000×*g* at 4 °C for 20 min.

SDS-PAGE was performed by loading isolated membrane proteins on a same chlorophyll basis on a 12.5% acrylamide resolving gel. After electrophoresis, proteins were transferred to a polyvinylidene difluoride (PVDF) membrane (Millipore-Sigma), blocked using 5% bovine serum albumin (Thermo-Fisher) for 2 h at room temperature, and then separately incubated with the primary rabbit antibody raised against Psb27 (Eaton-Rye lab) overnight at 4 °C. The horseradish peroxidase (HRP)-conjugated secondary antibody goat anti-rabbit IgG (H + L)-HRP conjugate (Bio-Rad) was diluted at 1:5000 in 1.5% BSA. Bands were visualized and quantified using chemiluminescence reagents (Millipore-Sigma) with a LI-COR Odyssey Fc (LI-COR Biotechnology) imager. Psb27 protein levels, on a per chlorophyll basis, in WT and OE27 are shown in Fig. S1C. OE27 has close to two times the Psb27 content of WT.

Fluorescence analysis

For non-photochemical quenching (NPQ) analysis using the Fluorocam 800MF (Photon System Instruments, Brno, Czech Republic), cells were grown to mid-log phase, harvested by centrifugation, washed in fresh BG11, and again centrifuged to pellet. The cell pellets were resuspended and diluted to $OD_{730} = 0.05$ in BG11 without antibiotics and spotted (2 µL) to BG11 plates without antibiotics. WT and mutant cells were allowed to grow under the same temperature and light conditions as liquid culture for 3 weeks before NPQ analysis.

Fluorescence emission over many flashes was recorded on a double-modulation fluorometer (Photon System Instruments, Brno, Czech Republic) with a built-in analyzing program, FluorWin, using a modified S-state program. 1000 flashes were delivered at 500 ms intervals over a period of 500 s. The sample concentration was adjusted to 5 µg/mL of Chl*a* in BG11. All samples were dark-adapted for 5 min at room temperature before the measurements. Instead of using 10 actinic flashes that advance S-state by each flash, 1000 flashes were used to test the Q_A^- reoxidation in three mutants versus WT. The charge recombination after the first flash and last flash were numerically deconvoluted. The fluctuation of *F*o, *F*m, *F*v was plotted against flash number.

To determine the charge transfer kinetics between Q_A^- and the plastoquinone bound at the Q_B-binding site, we employed a double exponential decay to fit the data in Table S2, where A_1 and A_2 are amplitudes, and T_1 and T_2 are time constants for the fast and intermediate components, respectively. To calculate respective decay $T_{1/2}$, the time constants were multiplied by Ln (2). *F*(t) is the fluorescence level, and *F*o is the base fluorescence.

$$F(t) - Fo = A1\exp\left(-\frac{t}{T1}\right) + A2\exp\left(-\frac{t}{T2}\right)$$

The first exponential (fast component) describes the charge transfer between the Q_A and plastoquinone bound at the Q_B site. The second exponential (intermediate component) describes plastoquinone exchange at the Q_B-binding site (Vass et al. 1999). Because the fluorescence decay was recorded for approximately 330 ms after the actinic flash, we did not consider a slow hyperbolic component ($T_{1/2}$ ranging in seconds) that would describe the $S_2Q_A^-$ charge recombination (Biswas and Eaton-Rye 2018). Residuals for the fits are shown in Fig S2.

Supplementary Information The online version contains supplementary material available at https://doi.org/10.1007/s11120-021-00895-3.

Acknowledgements We thank Dr. Julian Eaton-Rye for the kind gift of Psb27 antisera. This study was supported by U.S. Department of Energy (DOE), Office of Basic Energy Sciences, Grant DE-FG02-99ER20350 to H.B.P. H.L. was partially supported by DOE Grant DE-FG02-07ER15902.

Declarations

Conflict of interest The authors have no competing interests to declare.

References

Allen MM (1968) Simple conditions for growth of unicellular blue-green algae on plates(1, 2). J Phycol 4(1):1–4

Avramov AP, Hwang HJ, Burnap RL (2020) The role of Ca(2+) and protein scaffolding in the formation of nature's water oxidizing complex. Proc Natl Acad Sci U S A 117(45):28036–28045

Bentley FK, Luo H, Dilbeck P, Burnap RL, Eaton-Rye JJ (2008) Effects of inactivating psbM and psbT on photodamage and assembly of photosystem II in *Synechocystis* sp. PCC 6803. Biochemistry 47(44):11637–11646

Biswas S, Eaton-Rye JJ (2018) PsbY is required for prevention of photodamage to photosystem II in a PsbM-lacking mutant of *Synechocystis* sp. PCC 6803. Photosynthetica 56:200–209

Chen H, Zhang D, Guo J, Wu H, Jin M, Lu Q, Lu C, Zhang L (2006) A Psb27 homologue in *Arabidopsis thaliana* is required for

efficient repair of photodamaged photosystem II. Plant Mol Biol 61(4–5):567–575

Chen HYS, Bandyopadhyay A, Pakrasi HB (2018) Function, regulation and distribution of IsiA, a membrane-bound chlorophyll a-antenna protein in cyanobacteria. Photosynthetica 56(1):322–333

Davinagracia J (2021) The role of lipoprotein Psb27 in photosystem II biogenesis. Master of Science, University of Otago, Dunedin

Grasse N, Mamedov F, Becker K, Styring S, Rogner M, Nowaczyk MM (2011) Role of novel dimeric photosystem II (PSII)-Psb27 protein complex in PSII repair. J Biol Chem 286(34):29548–29555

Hou X, Fu A, Garcia VJ, Buchanan BB, Luan S (2015) PSB27: A thylakoid protein enabling *Arabidopsis* to adapt to changing light intensity. Proc Natl Acad Sci U S A 112(5):1613–1618

Huang G, Xiao Y, Pi X, Zhao L, Zhu Q, Wang T, Kuang T, Han G, Sui SF, Shen JR (2021). "Structural insights into a dimeric Psb27-photosystem II complex from a cyanobacterium *Thermosynechococcus vulcanus*." Proc Natl Acad Sci U S A (in Press).

Hwang HJ, Nagarajan A, McLain A, Burnap RL (2008) Assembly and disassembly of the photosystem II manganese cluster reversibly alters the coupling of the reaction center with the light-harvesting phycobilisome. Biochemistry 47(37):9747–9755

Ihalainen JA, D'Haene S, Yeremenko N, van Roon H, Arteni AA, Boekema EJ, van Grondelle R, Matthijs HC, Dekker JP (2005) Aggregates of the chlorophyll-binding protein IsiA (CP43') dissipate energy in cyanobacteria. Biochemistry 44(32):10846–10853

Jackson SA, Hervey JR, Dale AJ, Eaton-Rye JJ (2014) Removal of both Ycf48 and Psb27 in *Synechocystis* sp. PCC 6803 disrupts photosystem II assembly and alters Q(A)(-) oxidation in the mature complex. FEBS Lett 588(20):3751–3760

Kashino Y, Lauber WM, Carroll JA, Wang Q, Whitmarsh J, Satoh K, Pakrasi HB (2002) Proteomic analysis of a highly active photosystem II preparation from the cyanobacterium *Synechocystis* sp. PCC 6803 reveals the presence of novel polypeptides. Biochemistry 41(25):8004–8012

Kato Y, Nagao R, Noguchi T (2016) Redox potential of the terminal quinone electron acceptor QB in photosystem II reveals the mechanism of electron transfer regulation. Proc Natl Acad Sci U S A 113(3):620–625

Knoppova J, Sobotka R, Tichy M, Yu J, Konik P, Halada P, Nixon PJ, Komenda J (2014) Discovery of a chlorophyll binding protein complex involved in the early steps of photosystem II assembly in *Synechocystis*. Plant Cell 26(3):1200–1212

Komenda J, Knoppova J, Kopecna J, Sobotka R, Halada P, Yu J, Nickelsen J, Boehm M, Nixon PJ (2012) The Psb27 assembly factor binds to the CP43 complex of photosystem II in the cyanobacterium *Synechocystis* sp. PCC 6803. Plant Physiol 158(1):476–486

Krieger-Liszkay A, Fufezan C, Trebst A (2008) Singlet oxygen production in photosystem II and related protection mechanism. Photosynth Res 98(1–3):551–564

Kromdijk J, Glowacka K, Leonelli L, Gabilly ST, Iwai M, Niyogi KK, Long SP (2016) Improving photosynthesis and crop productivity by accelerating recovery from photoprotection. Science 354(6314):857–861

Liu H, Huang RYC, Chen J, Gross ML, Pakrasi HB (2011) Psb27, a transiently associated protein, binds to the chlorophyll binding protein CP43 in photosystem II assembly intermediates. Proc Natl Acad Sci USA 108(45):18536–18541

Liu H, Roose JL, Cameron JC, Pakrasi HB (2011) A genetically tagged Psb27 protein allows purification of two consecutive photosystem II (PSII) assembly intermediates in *Synechocystis* 6803, a cyanobacterium. J Biol Chem 286(28):24865–24871

Liu H, Chen J, Huang RY, Weisz D, Gross ML, Pakrasi HB (2013) Mass spectrometry-based footprinting reveals structural dynamics of loop E of the chlorophyll-binding protein CP43 during photosystem II assembly in the cyanobacterium *Synechocystis* 6803. J Biol Chem 288(20):14212–14220

Mamedov F, Nowaczyk MM, Thapper A, Rogner M, Styring S (2007) Functional characterization of monomeric photosystem II core preparations from *Thermosynechococcus elongatus* with or without the Psb27 protein. Biochemistry 46(18):5542–5551

Mohamed A, Jansson C (1989) Influence of light on accumulation of photosynthesis-specific transcripts in the cyanobacterium *Synechocystis* 6803. Plant Mol Biol 13(6):693–700

Niedzwiedzki DM, Tronina T, Liu H, Staleva H, Komenda J, Sobotka R, Blankenship RE, Polivka T (2016) Carotenoid-induced non-photochemical quenching in the cyanobacterial chlorophyll synthase-HliC/D complex. Biochim Biophys Acta 1857(9):1430–1439

Nowaczyk MM, Hebeler R, Schlodder E, Meyer HE, Warscheid B, Rogner M (2006) Psb27, a cyanobacterial lipoprotein, is involved in the repair cycle of photosystem II. Plant Cell 18(11):3121–3131

Ort DR, Merchant SS, Alric J, Barkan A, Blankenship RE, Bock R, Croce R, Hanson MR, Hibberd JM, Long SP, Moore TA, Moroney J, Niyogi KK, Parry MA, Peralta-Yahya PP, Prince RC, Redding KE, Spalding MH, van Wijk KJ, Vermaas WF, von Caemmerer S, Weber AP, Yeates TO, Yuan JS, Zhu XG (2015) Redesigning photosynthesis to sustainably meet global food and bioenergy demand. Proc Natl Acad Sci U S A 112(28):8529–8536

Roose JL (2008). Assembly and function of cyanobacterial photosystem II, Ph.D thesis. Washington University, St. Louis, MO.

Roose JL, Pakrasi HB (2008) The Psb27 protein facilitates manganese cluster assembly in photosystem II. J Biol Chem 283(7):4044–4050

Rutherford AW, Osyczka A, Rappaport F (2012) Back-reactions, short-circuits, leaks and other energy wasteful reactions in biological electron transfer: redox tuning to survive life in O(2). FEBS Lett 586(5):603–616

Singh H (2017) The role of the low-molecular-weight proteins of the CP43 pre-assembly complex of photosystem II. Doctor of Philosophy, University of Otago, Dunedin

Suga M, Akita F, Hirata K, Ueno G, Murakami H, Nakajima Y, Shimizu T, Yamashita K, Yamamoto M, Ago H, Shen JR (2015) Native structure of photosystem II at 1.95 a resolution viewed by femtosecond X-ray pulses. Nature 517(7532):99–103

Vass I, Kirilovsky D, Etienne AL (1999) UV-B radiation-induced donor- and acceptor-side modifications of photosystem II in the cyanobacterium *Synechocystis* sp. PCC 6803. Biochemistry 38(39):12786–12794

Veerman J, Bentley FK, Eaton-Rye JJ, Mullineaux CW, Vasil'ev S, Bruce D (2005) The PsbU subunit of photosystem II stabilizes energy transfer and primary photochemistry in the phycobilisome-photosystem II assembly of *Synechocystis* sp. PCC 6803. Biochemistry 44(51):16939–16948

Wilson A, Ajlani G, Verbavatz JM, Vass I, Kerfeld CA, Kirilovsky D (2006) A soluble carotenoid protein involved in phycobilisome-related energy dissipation in cyanobacteria. Plant Cell 18(4):992–1007

Wilson A, Punginelli C, Gall A, Bonetti C, Alexandre M, Routaboul JM, Kerfeld CA, van Grondelle R, Robert B, Kennis JT, Kirilovsky D (2008) A photoactive carotenoid protein acting as light intensity sensor. Proc Natl Acad Sci U S A 105(33):12075–12080

Zabret J, Bohn S, Schuller SK, Arnolds O, Moller M, Meier-Credo J, Liauw P, Chan A, Tajkhorshid E, Langer JD, Stoll R, Krieger-Liszkay A, Engel BD, Rudack T, Schuller JM, Nowaczyk MM (2021) Structural insights into photosystem II assembly. Nat Plants 7(4):524–538